Molecular BioSystems

PAPER

View Article Online
View Journal

Cite this: DOI: 10.1039/c5mb00525f

Effect of oncogene activating mutations and kinase inhibitors on amino acid metabolism of human isogenic breast cancer cells†

Eung-Sam Kim,[ab] Animesh Samanta,[a] Hui Shan Cheng,[a] Zhaobing Ding,[a] Weiping Han,[a] Luisella Toschi[c] and Young Tae Chang*[ad]

Received 3rd August 2015,
Accepted 3rd October 2015

DOI: 10.1039/c5mb00525f

www.rsc.org/molecularbiosystems

We investigated the changes in amino acid (AA) metabolism induced in MCF10A, a human mammary epithelial cell line, by the sequential knock-in of K-Ras and PI3K mutant oncogenes. Differentially regulated genes associated to AA pathways were identified on comparing gene expression patterns in the isogenic cell lines. Additionally, we monitored the changes in the levels of AAs and transcripts in the cell lines treated with kinase inhibitors (REGO: a multi-kinase inhibitor, PI3K-i: a PI3K inhibitor, and MEK-i: a MEK inhibitor). In total, 19 AAs and 58 AA-associated transcripts were found to be differentially regulated by oncogene knock-in and by drug treatment. In particular, the multi-kinase and MEK inhibitor affected pathways in K-Ras mutant cells, whereas the PI3K inhibitor showed a major impact in the K-Ras/PI3K double mutant cells. These findings may indicate the dependency of AA metabolism on the oncogene mutation pattern in human cancer. Thus, future therapy might include combinations of kinase inhibitors and drug targeting enzymes of AA pathways.

Introduction

Since Otto H. Warburg's observation of anomalous metabolism in cancer cells, the altered cellular metabolism has been emerging as a hallmark of cancer.[1–3] Many cancer cells are found to favor aerobic glycolysis and anaplerotic reactions in order to satisfy the demand for energy and building blocks such as nucleotides, amino acids, and lipids for cell growth and survival.[4,5] Recent reports have attributed the reprogrammed metabolism of cancer cells to activated oncogenes or altered tumor suppressors.[6,7] Therefore, targeting metabolic pathways in cancer cells has been suggested to improve the efficacy of anti-tumor therapeutics.[8] Thus, it becomes important to understand the effect of cancer genetic lesions on cellular metabolic processes aiming at the improvement of anti-tumor drugs.

It is well-known that intracellular amino acids not only act as basic building units of proteins but also participate in the metabolic regulation in cells. Under amino acid starvation, both proteasomal degradation and autophagy are engaged to maintain appropriate amino acid levels in cells.[9–11] Moreover, the blood concentration of amino acids provides a potential diagnostic parameter in diseases such as diabetes, hypermetabolic syndrome and cancer.[12–14] Since malignant tumor cells require more amino acids to synthesize proteins or to provide amino acid-derived metabolites, amino acid profiles obtained from extracellular fluids such as blood plasma, saliva or urine enable one to screen the progress of cancer.[15–17] Recently Gu *et al.* reported that plasma free amino acid (PFAA) profiles of cancer patients were dynamically altered during the perioperative period.[18] The finding that the PFAA profile of pancreatic cancer patients was significantly different from that of healthy subjects demonstrated that the PFAA profiling might be developed as a promising diagnostic method for the early detection of pancreatic cancer with poor prognosis.[19] Cheng *et al.* applied this profiling approach to saliva instead of blood for the early diagnosis of breast cancer. It is expected that the combination of amino acid profiles and conventional tumor markers may further improve the outcome of cancer diagnosis and prognosis.[20]

The impact of anticancer drugs such as taxol on cellular metabolism can be evaluated by monitoring the change of intracellular amino acids.[21] In the attempt to investigate the amino acid metabolism in a cancer cell model, we used immortalized breast epithelial MCF10A cells harboring the sequential knock-in of oncogenic K-Ras (G12V) and PI3K (E545K) mutations.[22,23] The isogenic MCF10A cell lines, which include parental, K-Ras

[a] Singapore Bioimaging Consortium, Agency for Science, Technology and Research (A*STAR), 11 Biopolis Way, #02-02 Helios Building, 138667, Singapore
[b] Department of Biological Sciences, Chonnam National University, Gwangju, Korea
[c] Global Drug Discovery, Therapeutic Research Group Oncology/Gynecological Therapies, Tumor Metabolism, Bayer Pharma AG, Berlin, Germany
[d] Department of Chemistry & MedChem Program of Life Sciences Institute, National University of Singapore, 117543, Singapore. E-mail: chmcyt@nus.edu.sg

† Electronic supplementary information (ESI) available. See DOI: 10.1039/c5mb00525f

(G12V) and K-Ras (G12V)/ PI3K (E545K) knock-in, enable one to recapitulate the main steps towards oncogenic transformation within their intact genetic background.[24] As extensively reported, K-Ras and PI3K activating mutations have been identified in the majority of cancer types. In particular, PI3K (E545K) mutation has been detected in up to 20% of breast cancer patients.[22,25]

Thus, the aim of this work is, on one hand, to investigate the changes of amino acid levels in the process of oncogenic transformation, and, on the other hand, to address the impact of anti-cancer drugs such as kinase inhibitors on amino acid metabolism and on the expression of the genes in the associated pathways.

Experimental

Materials and methods

Chemicals. All chemicals and solvents of reagent grade were purchased from Sigma-Aldrich (St. Louis, MO, USA), unless otherwise mentioned. The reagents used in HPLC analysis are HPLC-grade. The signaling inhibitory chemicals were provided by Bayer Healthcare. Ultra-pure water (18.2×10^6 Ω cm) for the preparation of aqueous solutions was supplied by a Milli-Q purification system (Millipore). Ortho-phthalaldehyde (OPA) was purchased from Agilent.

Drug information. Three kinase inhibitors were provided by Bayer Health Care. REGO, PI3K-i and MEK-i are known to inhibit multiple kinases, PI3K, and MEK, respectively[26,27] (S.1, ESI†). In the case of REGO (Stivarga™), it was approved by FDA in 2012 and called as Regorafenib to treat metastatic colorectal cancer.[28] The 10 mM stock of each drug was prepared according to the provider's guidance and stored in the dark at room temperature (RT). REGO and MEK-i were dissolved in anhydrous DMSO. PI3K-i was dissolved in DMSO supplemented with 10 mM trifluoroacetic acid. The volume ratio of a drug solution to be added to the cell culture was set to 0.05% to minimize the toxicity of the stock solvent. For the non-treated control, only the solvent was added to the cell culture.

Cell culture. The three MCF-10A cell lines (HD PAR-003, HD 101-004 and HD 201-002) were provided by Horizon Discovery (Cambridge Research Park, Cambridge, United Kingdom). Since the HD 101-004 and HD 201-002 cells contain the targeted knock-in mutants of K-Ras$^{(G12V)}$ and K-Ras$^{(G12V)}$/PI3Ka$^{(E545K)}$, respectively, compared to their parental wild-type (WT) cell, HD PAR-003, the three cell lines are renamed WT, K-Ras, and K-Ras/PI3K in this work. Cells were grown in DMEM : F12 (1 : 1) medium supplemented with 5% horse serum, 20 ng ml^{-1} epidermal growth factor (EGF), 10 μg ml^{-1} insulin, 0.5 μg ml^{-1} hydrocortisone, 0.1 μg ml^{-1} cholera toxin, 100 U ml^{-1} penicillin, and 100 μg ml^{-1} streptomycin. Cells were maintained at 37 °C with 5% CO_2 in a humidified atmosphere. For sample collection (10^7 cells in each sample), the cells were washed with phosphate buffered saline (PBS) solution twice and detached with 0.25% trypsin/EDTA (GIBCO). The harvested cells were counted in an automatic cell counter (Mini Automated Cell Counter, ORFLO). The cell density under drug treatment was nearly 70%.

MTS assay for determination of IC_{50} values of kinase inhibitors. MCF-10A cells (3000 cells per well, 60 μl per well) were seeded on clear and flat-bottomed 96-well plates with blank wells containing media only. At 24 h after cell seeding, the drug-containing medium (50 μl per well) was added to each well. After an additional 48 h, 20 μl of MTS reagent (Promega) was added to each well. The 96-well plate was incubated for 1 h prior to reading absorbance at 490 nm in a plate reader (Molecular Devices).

HPLC for profiling intracellular amino acids

Methanol extraction. The extraction of intracellular free amino acids was performed by slightly modifying the procedure of a previous study.[22] Briefly, the cell pellet was resuspended in 0.5 ml of 100% methanol and frozen in liquid nitrogen and then thawed on ice. The cell vial was vortexed for 30 s and centrifuged at 800 × *g* for 5 min. The supernatant was collected and the pellet was resuspended in 0.5 ml of 100% methanol for another freeze–thaw cycle. Ultrapure water (0.3 ml) at 4 °C was added to the collected supernatant. The supernatant was subjected to freeze–thaw cycle followed by centrifugation at 15 000 × *g* for 5 min. The final supernatant was dried at 35 °C in a SpeedVac concentrator overnight. The schematic diagram of this extraction procedure is presented in S.3 (ESI†).

Ortho-phthalaldehyde (OPA) derivatization. The vacuum-dried extract in an e-tube was dissolved in 200 μl of 0.1 M HCl and filtered through a 3 kDa-MWCO cellulose membrane filter (Millipore) following centrifugation at 20 000 × *g* for 15 min at 4 °C. In order to obtain a labeling solution, 10 μl of 0.1 M iodoacetic acid solution (18 mg per 1.0 ml DDW), 10 μl of 100 μM norvaline solution and 10 μl of OPA solution (10 mg ml^{-1} OPA and 3-MPA in 0.4 M borate buffer) were added to 10 μl of the dissolved extract solution just before injection into an HPLC column. Norvaline (abbreviated as Nva) represented an amino acid used as an internal standard for peak normalization.

Reversed-phase HPLC separation of OPA-labeled amino acids

The separation was performed at 40 °C on a Gemini-NX 5 μm C_{18} 100Å column (Phenomenex) installed in an HPLC (Dionex Ultimate 3000) using a gradient run at 1.0 ml of 40 mM $NaHPO_4$ (pH 7.8 at RT, adjusted with H_3PO_4) (A solution) and methanol/acetonitrile/water (45 : 45 : 10 by volume) (B solution) from 0% B to 57% B in 57 min (S.4, ESI†). For fluorescence detection, the wavelength was set up at 345 nm (excitation) and 455 nm (emission). All HPLC solutions were filtered using a 0.22 μm membrane filter (Millipore) before use. Because of the instability of the OPA-amino acid derivative, HPLC separation was performed immediately following pre-column derivatization.

Quantification of amino acids. Each amino acid peak in a chromatogram was identified and assigned by a standard chromatogram for the amino acid. The standard curve and calibration equation for the 19 amino acids subject to the identical HPLC condition were established as summarized in S.5 (ESI†). When each calibration curve is fitted to a line with zero offset, the correlation coefficient is between 0.95 and 0.99. The baseline of a chromatogram was determined and the area of each assigned peak was obtained and normalized by that of

the Nva peak. The concentration of each amino acid in the chromatogram was estimated using the calibration curve. The amount of an individual amino acid was divided by the total amino acid amount in the chromatogram to calculate the percentage portion of each amino acid.

Quantification of intracellular glutathione (GSH) levels. As recommended by the manufacturer's guide (Sigma-Aldrich), the pellet of 5×10^6 cells was suspended in 80 μl of 1× lysis buffer and incubated on ice for 15 min. The supernatant obtained from the centrifugation (16 000 × *g*, 10 min, 4 °C) of the resuspended cell pellet was placed in the microwell of a 96-well plate. The assay buffer, GST enzyme, and substrate solution were added to the well and incubated for 1 h at 37 °C. Under the excitation at 390 nm, the fluorescence signal at 478 nm in the well was obtained in a plate reader (Molecular Devices). The standard curve for GSH and the estimated volume of individual cells were used to obtain the intracellular GSH concentration from the fluorescence level.

Gene expression profiling with qPCR arrays. Human amino acid metabolism I/II PCR arrays of 96-well plate format were purchased from QIAGEN. The drugs were applied for 24 h prior to cell harvest. The total RNA was extracted from freshly harvested cells using the RNeasy kit (QIAGEN) and converted into cDNA using the RT2 First Strand Kit (QIAGEN). The PCR template was combined with SYBR Green qPCR Master Mix before adding equal aliquots (*i.e.* 25 μl) of this mixture to each well of each PCR array plate containing the predispensed gene-specific primer sets. The quantitative real-time PCR was carried out in a thermocycle machine (StepOnePlus, Life Technology). The threshold cycle (Ct) value for amino acid-associated genes and housekeeping genes was determined to calculate fold changes (ΔCt) in gene expression. A valid-flagged gene was defined as follows: Ct value below 25, expression change at least 2-fold compared to control condition.

Statistics. The data were obtained from three independent experiments and are expressed as mean ± S.D. The results were compared using Student's *t*-test. Statistical significance was considered at $p < 0.05$.

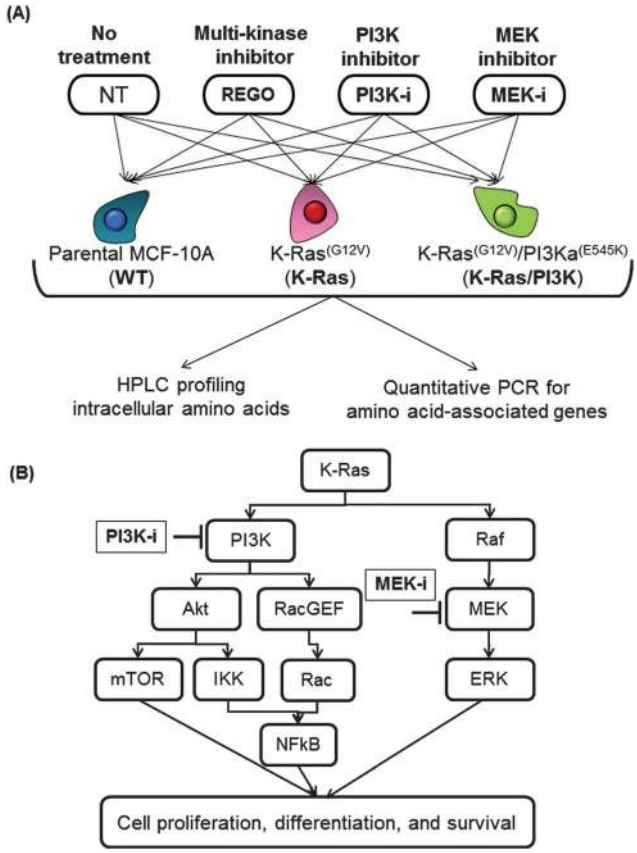

Fig. 1 Cell models and experiment design. (A) The targeted knock-in of oncogenic K-Ras(G12V) and PI3K(E545K) generates cancer-recapitulating K-Ras and K-Ras/PI3K cells. Three kinds of kinase inhibitors (REGO, PI3K-i, and MEK-i) were applied to the three cell lines. The intracellular amino acids and total RNA extracted from untreated and drug-treated cells were analysed by reversed-phase HPLC and quantitative PCR, respectively. (B) Scheme of K-Ras signaling pathways indicating the respective drug targets.

Results and discussion

Part 1: changes in intracellular amino acid (AA) levels

In order to investigate the effect of the two oncogenes and three kinase inhibitors on AA metabolism in MCF-10A cells, we compared intracellular AA levels of WT, K-Ras, and K-Ras/PI3K cells (Fig. 1) under vehicle and drug treatment at 24 h and 48 h. We employed three kinds of kinase inhibitors: REGO, a multi-kinase inhibitor; PI3K-i, a PI3K inhibitor; and MEK-i, a pan-MEK inhibitor.[20,21] The treatment concentration of a drug was set to its IC_{50} value determined from the MTS assay (S.6, ESI†).

The OPA pre-column derivatization followed by HPLC and fluorescence detection could separate and quantify 19 intracellular free AAs extracted from the three MCF-10A cell lines. The HPLC separation provided reproducible chromatograms showing distinctive peaks for 19 AAs and three unidentified ones (S.7, ESI†). The first and the last AAs in a chromatogram were Asp and Lys, respectively. Since Pro with no amino group cannot be labeled with the amine-reactive OPA, the AA was detected in the HPLC profile. The 19 AAs were classified into three groups based on their relative fractions in the total AA extracted from untreated WT cells: major, intermediate, minor AAs. Glu (*ca.* 38%), Gln (*ca.* 14%), Asp (*ca.* 10%), and Cys (*ca.* 9%) were included in the major AAs (Fig. 2A and 3A). The intermediate group (1 to 5%) contained 10 amino acids: Gly, Thr, Arg, Ala, Tyr, Val, Phe, Ile, Leu, and Lys. The other five AAs, *i.e.* Asn, Ser, His, Met, and Trp, with less than 1% were set as minor AAs.

The difference in AA levels between WT and K-Ras cells were marginal when they were cultured for 24 h without any inhibitors. K-Ras/PI3K cells under the same culture condition had significantly higher Cys level (*ca.* 13%) than WT and K-Ras cells (*ca.* 7%). When the untreated cells were analyzed at 48 h, the difference in some AA levels became more apparent. The mutant cells had lower levels of Glu compared to the WT cell. The level of Gln and Cys in K-Ras/PI3K was further increased in comparison to that at 24 h. When we measured reduced GSH

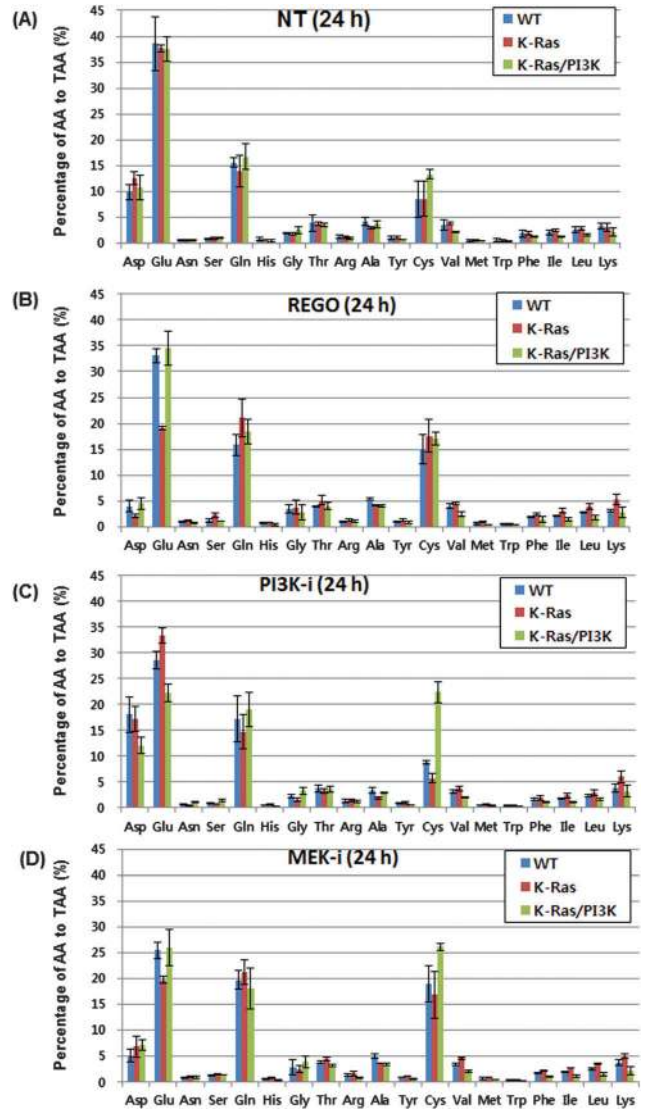

Fig. 2 Quantification of intracellular amino acids in the three cell lines at 24 h drug treatment. OPA-labeled amino acids extracted from WT, K-Ras, and K-Ras/PI3K cells were separated and quantified by HPLC and fluorescence detection, respectively. (A) Amino acid levels of cells with no drug treatment. (B) Amino acid levels of cells with REGO treatment. (C) Amino acid levels of cells with PI3K-i treatment. (D) Amino acid levels of cells with MEK-i treatment. The order of appearance of amino acids on the *x*-axis reflects their respective retention time in the chromatogram. Each amino acid level is normalized to total amino acids (mean ± S.D., n = 3).

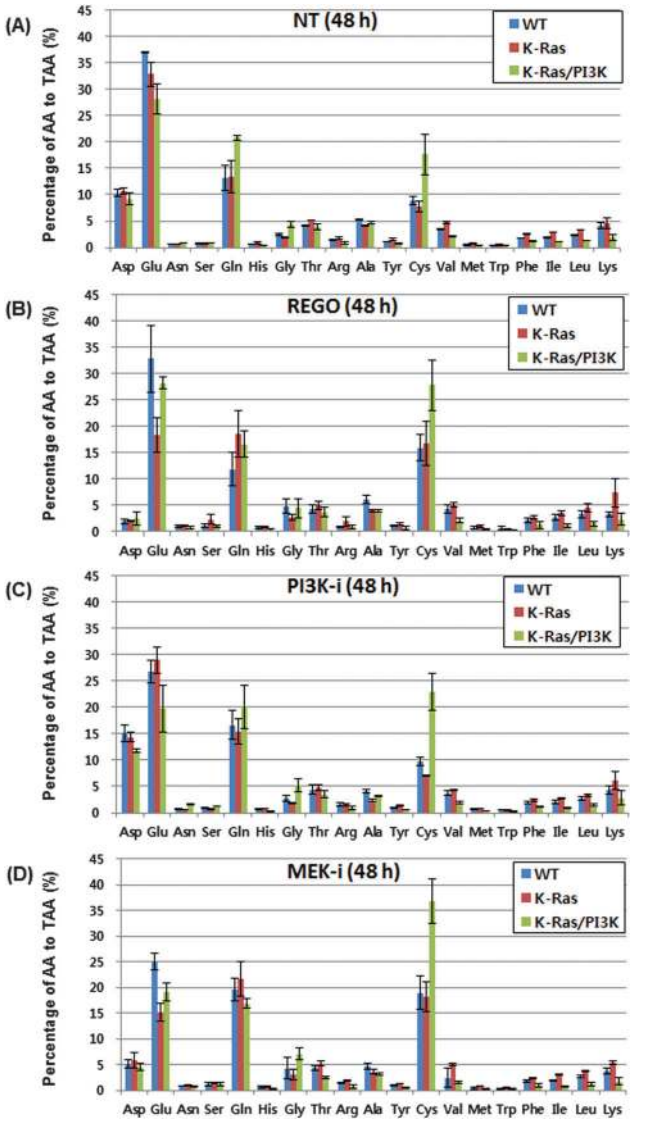

Fig. 3 Quantification of intracellular amino acid levels in the three cell lines at 48 h drug treatment. (A), (B), (C) and (D) as in Fig. 2. Analysis and abbreviations as in Fig. 2.

levels in the three types of cells (S.8, ESI†), K-Ras/PI3K cells showed a 1.46-fold higher GSH level compared to WT cells. The difference in the GSH level between K-Ras and WT cells was ignorable. Since GSH is composed of three AAs, Gly, Cys, and Glu, the upregulated AAs (Gly and Cys) in K-Ras/PI3K cells can be associated with the higher level of GSH in the cells in comparison to the other cells.

The treatment with the kinase inhibitors introduced more significant changes in the major AAs and some of intermediate AAs such as Gly and Lys. On the other hand, most of minor AAs remained unchanged under drug treatment. The treatment with REGO, a multi-kinase inhibitor, decreased Asp level significantly in the three cell lines at 24 h and 48 h. In contrast, the Cys level increased up to 15% under the same condition (Fig. 2B and 3B). Interestingly, the REGO treatment in K-Ras cells resulted in a decrease of Glu level to half of the untreated level while a 2-fold increase in the Lys level was observed. The treatment with PI3K-i led to an overall moderate increase of Asp and Lys levels as well as to the overall decrease of Glu levels in the three cell lines compared to the untreated cells (Fig. 2C and 3C). In addition, the PI3K-i induced a significant increase of the Cys level in K-Ras/PI3K cells whereas in the other cell lines no noticeable change of Cys level was detected.

The treatment with MEK-i resulted in a decrease of Asp and Glu levels in the three cell lines while Cys levels increased 2-fold compared to untreated cells (Fig. 2D and 3D). The MEK-i increased the relative level of Cys to *ca.* 37% in K-Ras/PI3K cells, which became

the most abundant AA in this cell line. In contrast, the most abundant AA in other profiles was Glu regardless of cell type or drug treatment. In order to address the change in amino acid profiles among the three cell lines, we set as differentially regulated AA any AA showing more than 1.5-fold change in its level when comparing either mutant *vs.* WT cells or treated *vs.* untreated condition. Since the mean and standard deviation of all coefficients of variation of individual AA levels are 0.17 and 0.13, respectively, the 1.5-fold criterion for the significant fold change of AAs seems to be reasonable considering the two-sigma.

In the first part of the study, amino acid levels of K-Ras and K-Ras/PI3K cells were compared with those of WT cells to examine the effect of oncogene knock-in on AA metabolism. The upregulated or downregulated amino acids in K-Ras and K-Ras/PI3K cells are listed in Table S1 (ESI†). When the AA levels of K-Ras cells were compared with those of WT cells, no AA showed a significant fold change at 24 h. However, three AAs (Try, Trp, and Ile) were upregulated at 48 h in K-Ras cells while no AA was down-regulated.

In K-Ras/PI3K cells at 24 h, Cys was increased and seven AAs were decreased. At 48 h in K-Ras/PI3K cells, three AAs (Gln, Gly, and Cys) were upregulated and eight downregulated, which included six AAs (His, Try, Phe, Ile, Leu, and Lys) already decreased at 24 h. Interestingly, the three AAs (Trp, Tyr, and Ile) upregulated in K-Ras cells at 48 h turned out to be down-regulated in K-Ras/PI3K cells.

Thus, the opposite regulation of AAs might imply that the additional knock-in of PI3K mutant oncogenes into K-Ras cells induces a drastic rearrangement of AA metabolism in K-Ras/PI3K cells compared to K-Ras cells. Thus, the change of AA levels in WT, K-Ras, and K-Ras/PI3K cells suggests that the sequential knock-in of the two oncogenes into WT cells can result in extensive reprogramming of AA metabolism.

In the second part, the impact of the three kinase inhibitors on AA levels was addressed in WT cells compared to the untreated condition (Table S2 and S.10, ESI†). Under REGO treatment at 24 h, five AAs (Asn, Ser, Gly, Cys, and Met) were upregulated and Asp was downregulated in comparison to the untreated WT cells. At 48 h five AAs (Asn, Gly, Cys, Met, and Trp) were upregulated and one (Asp) slightly downregulated. PI3K-i treatment at both time points induced no detectable changes in AA levels except for Asp upregulation at 24 h. Under MEK-i treatment at 24 h, four AAs (Ser, Gly, Cys, and Met) were upregulated and two AAs (Asp and Glu) downregulated. At 48 h of MEK-i treatment the AA profile remained almost unchanged compared to 24 h treatment. In summary, REGO and MEK-i induced comparable AA changes at both time points in WT cells. On the other hand, PI3K-i had an overall modest impact on AA metabolism except for Asp upregulation at 24 h.

In the third part of the study, we analyzed the AA profiles in drug-treated K-Ras and K-Ras/PI3K cells in comparison to the corresponding untreated cells (Table S3, Fig. 4, and S.9, ESI†). REGO treatment had a major impact on K-Ras cells, since several AAs were upregulated at both time points. On the other hand, only Cys was increased under REGO treatment at 48 h in K-Ras/PI3K cells. Considering the number of AAs affected by the drugs in the mutant cell lines, it appeared that PI3K-i and MEK-i had a major impact on AA regulation in the cells expressing the respective target mutations. In line with this observation, the PI3K-i modulated five AAs (Asn, Ser, Cys, Lys and Glu) in K-Ras/PI3K cells, whereas the same inhibitor had only a minor impact on AA levels in K-Ras cells. Interestingly, Lys increase and Ala decrease under PI3K-i treatment were detected in both mutant cell lines, suggesting potential common AA pathways activated by the oncogenes. As previously pointed out, MEK-i affected consistently more AAs in K-Ras cells as compared to K-Ras/PI3K cells. Interestingly, four AAs (Cys, Gly, Asp and Glu) appeared to be commonly regulated in all three cell lines, suggesting an impact of MEK-i on AA pathways shared by oncogene- and non-transformed cells. In general, the AA profile at both time points was very similar between untreated WT and K-Ras cells. In line with this observation, REGO and MEK-i induced similar AA patterns in WT and K-Ras cells. On the other hand, REGO and MEK-i displayed a minor impact on AA metabolism in K-Ras/PI3K cells. Thus, it can be speculated that PI3K mutant knock-in activates additional AA pathways beyond the spectrum targeted by REGO and MEK-i. In this line of evidence, PI3K-i has a major effect on the AA pattern in K-Ras/PI3K cells, leaving WT and K-Ras cells almost unaffected.

Part 2: regulation of transcripts of amino acid-associated enzymes

Quantitative PCR was employed to investigate the transcript level of 158 genes known to be associated with AA metabolism and, therefore, potentially affected by oncogene expression and by kinase inhibitors. Nine genes were identified as differentially expressed genes (DEGs) in untreated K-Ras and K-Ras/PI3K cells compared to untreated WT cells. Under drug treatment in the three cell lines, the total number of DEGs raised to 57 (listed in S.10 and 11, ESI†). Forty DEGs induced by oncogenes or drugs could be classified into six metabolic pathways (http://www.kegg.jp/kegg/pathway.html#amino): Arg/Asp/polyamine/AMP metabolism (Pathway 1), Gln/Glu metabolism (Pathway 2), Cys/Met metabolism (Pathway 3), Ser/Gly/Thr metabolism (Pathway 4), lysine catabolism (Pathway 5), and β-oxidation of fatty acids (Pathway 6).

Among oncogene-induced DEGs (Table S4, ESI†), ODC1, ASNS, BHMT, PHGDH and PSAT1 were upregulated in K-Ras/PI3K cells while GCAT and AASS involved in Thr and Lys catabolism, respectively, were downregulated. The four upregulated genes (ODC1, ASNS, PHGDH, and PSAT1) in Pathways 1, 2, and 4 of K-Ras/PI3K cells might contribute to cell growth and energy supply, since these genes are involved in the synthesis of growth factors, cell material and in ATP production.

In K-Ras compared to WT cells no major changes of gene expression occurred, except for the downregulation of ASNS, BHMT and ACADM. BHMT, involved in Cys metabolism, was downregulated in K-Ras cells whereas it was upregulated in K-Ras/PI3K cells. Since this enzyme is known to convert homocysteine to Met, the gene expression does not correlate with the high Cys level in K-Ras/PI3K cells.

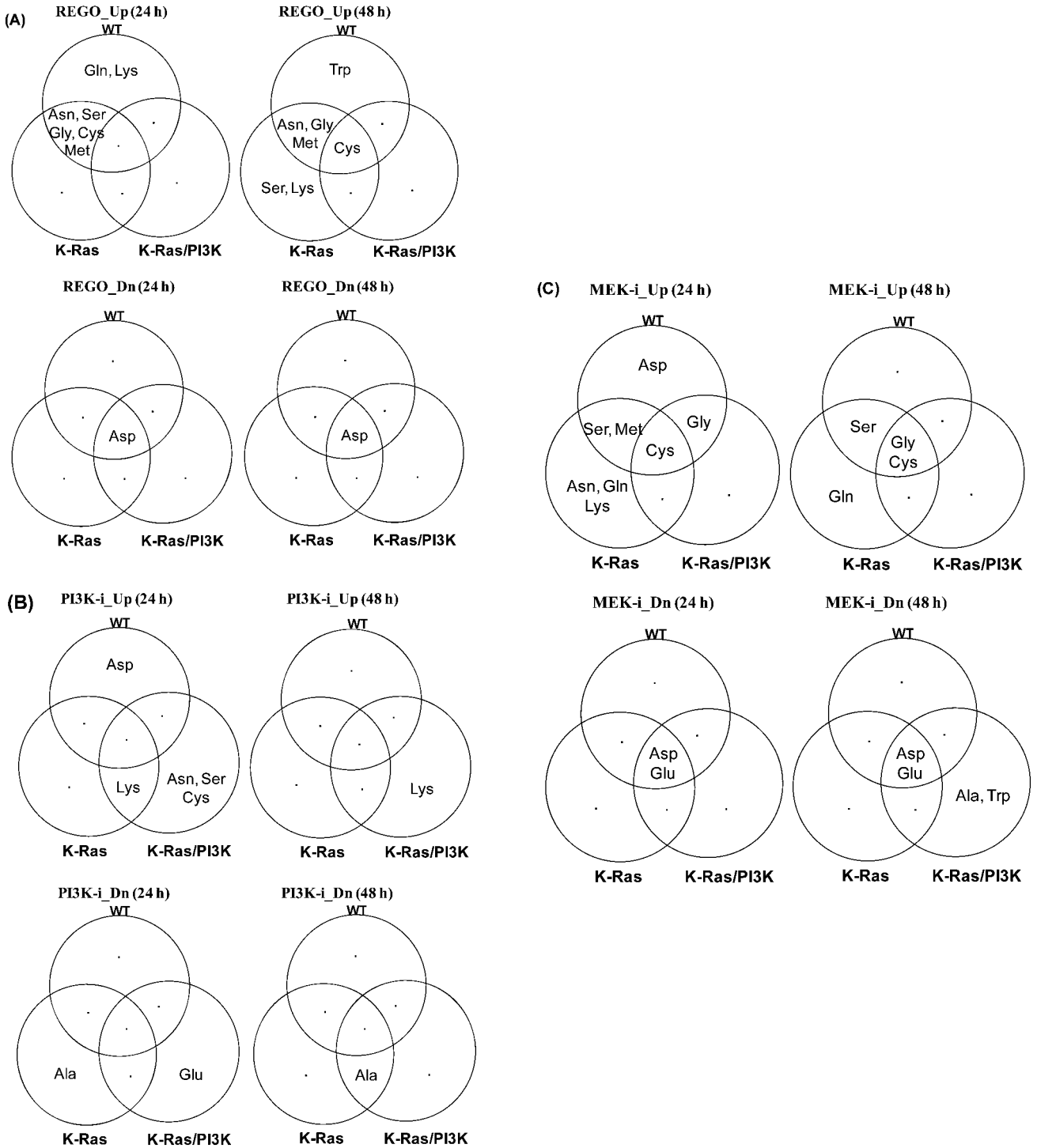

Fig. 4 Amino acids with significant changes in the levels upon inhibitor treatment in the three cell lines. (A) Upregulated or downregulated amino acids in cells under 24 h and 48 h treatment with REGO. (B) Upregulated or downregulated amino acids in cells under 24 h and 48 h treatment with PI3K-i. (C) Upregulated or downregulated amino acids in cells under 24 h and 48 h treatment with MEK-i.

Under treatment with the kinase inhibitors, most DEGs in the six pathways were downregulated, while a few genes were upregulated in a cell line-dependent manner. Pathway 1 (Fig. 5A) contains differentially expressed enzymes within the Arg/Asp/polyamine/AMP metabolism. Their gene expression pattern is shown in Table S5 (ESI†). The MEK-i treatment downregulated ADSL, ADSS, ASNS, and ODC1 in the three cell lines. In particular, ASNS was significantly decreased by the three drugs in K-Ras/PI3K cells. In these cells PI3K-i had a major impact on ASNS level displaying a 20-fold downregulation. Nevertheless, the general downregulation of ASNS and GOT1 by PI3K-i might have a differential effect on Asp level in each cell

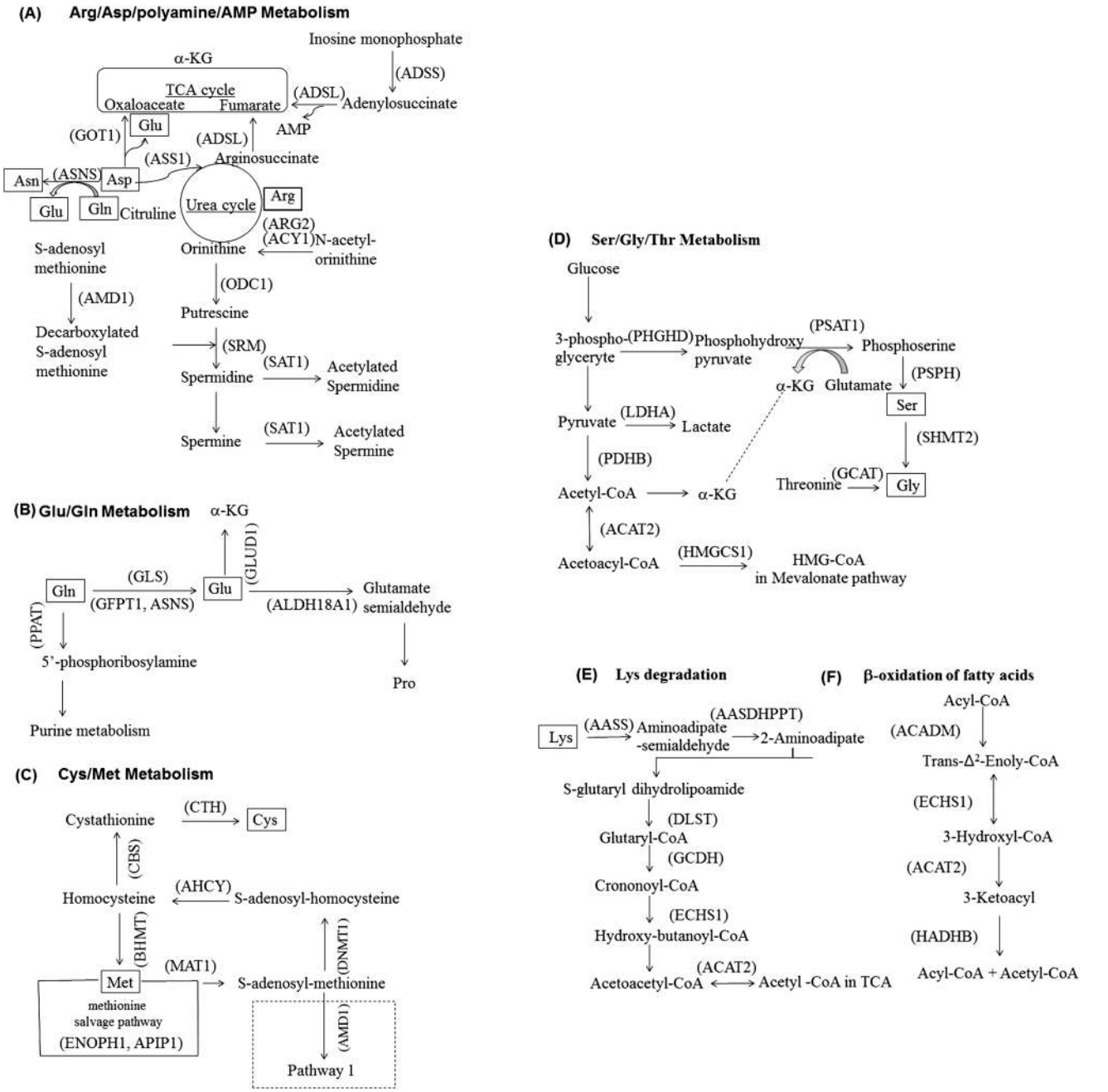

Fig. 5 Metabolic pathways of the differentially expressed genes (DEGs). (A) Arg/Asp/polyamine/AMP metabolism. (B) Glu/Gln metabolism. (C) Cys/Met metabolism. (D) Ser/Gly/Thr metabolism. (E) Lys degradation. (F) β-Oxidation of fatty acids.

line. In fact, PI3K-i raises Asp level in WT cells, whereas in the mutant cells Asp level is not affected under the same treatment. It might be postulated that the mutant cells in response to PI3K-i enable compensatory mechanisms to maintain Asp level unchanged.

The DEGs in Pathway 2 (Fig. 5B) are depicted in Table S6 (ESI†). GLUD1 was clearly upregulated in WT cells treated with PI3K-i or MEK-i while it showed no significant changes in the mutant cells under any kinase inhibitor treatment. The upregulation of GLUD1, the key enzyme converting Glu to α-KG, is in good correlation with the decrease of Glu level in WT cells treated with PI3K-i and MEK-i. Similarly, REGO and MEK-i treatment led to a 2-fold decrease of Glu level in K-Ras cells, which in this cell line might result from the drug-induced downregulation of GLS, the key enzyme in the conversion of Gln into Glu.

The gene expression pattern of enzymes in Pathway 3, Cys/Met metabolism (Fig. 5C), is shown in Table S7 (ESI†). Overall, no major impact of the kinase inhibitors was detected in the gene expression from this pathway in any cell line. The almost unchanged expression profile might also explain the marginal effect of any condition or treatment on Cys and Met levels.

Pathway 4 (Fig. 5D) depicts a metabolic pathway for synthesis or consumption of Ser, Gly, and Thr. The associated enzymes are shown in Table S8 (ESI†). The treatment with the kinase inhibitors in the three cell lines had a very weak outcome on the gene expression from this pathway. The only exception was REGO treatment in K-Ras cells. Under REGO treatment, PHGDH and PSAT1 were upregulated, whereas LDHA and PDHB were decreased. Thus, the differential regulation of these four genes might switch the conversion of glucose-derived 3-phosphoglycerate into Ser and might account for the significant increase of Ser level (see Table S3, ESI†).

The enzymes involved in Lys catabolism are shown in Fig. 5E and Table S9 (ESI†). Overall, none of the genes was upregulated under the drug treatment. The general downregulation induced by the drugs in this pathway might account for the increased level of Lys particularly in mutant cells. Table S10 (ESI†) lists the DEGs associated with β-oxidation of fatty acids into acetyl-CoA as depicted in Fig. 5F. As in the two previous pathways, no major differential regulation was visible in the genes from this pathway. Interestingly, in mutant cells PI3K-i and MEK-i treatment induced downregulation of ACAT2 which plays an essential role in the production of acetyl-CoA, a molecule connected to Ser/Gly/Thr metabolism and Lys catabolism and a building block in fatty acid synthesis.

In summary, our results show that the knock-in of K-Ras and PI3K mutant oncogenes induces a differential gene expression within the major metabolic pathways. K-Ras and K-Ras/PI3K cells exhibit 4 and 8 DEGs, respectively, compared to WT cells. Interestingly, there was no common gene among the two sets of DEGs, taking into account that K-Ras is expressed in both mutant cell lines. Moreover, there were very few commonly regulated genes within the 58 DEGs in the drug-treated cell lines. Along this observation, the ratio of exclusive *vs.* common genes in WT compared to mutant cells might provide an assessment of tumor-selective effects of the drugs (Fig. 6 and S.12, ESI†).

In these terms, REGO treatment affected more specifically K-Ras than K-Ras/PI3K cells (S.12, ESI:† 32/3 genes K-Ras *vs.* 10/3 genes K-Ras/PI3K cells). In contrast, the PI3K-i effect clearly dominated in K-Ras/PI3K cells (S.12, ESI:† 20/4 genes K-Ras/PI3K *vs.* 5/4 genes K-Ras cells), potentially supporting the target-selective activity in these mutant cells. MEK-i treatment provided similar ratios in the mutant compared to WT cells, potentially reflecting the fact that MEK resides further downstream from K-Ras and PI3K. Overall, this preliminary analysis suggests potential correlations between AA levels and the expression of the associated metabolic genes in response to oncogene transformation and kinase inhibitor treatment. Nevertheless, future work should address changes potentially affecting the protein level and post-translational modifications known to impact the enzyme activity. Moreover, a more comprehensive bioinformatics analysis will contribute to disclose the complex interplay between AA metabolism and survival pathways in cancer cells. Although our intracellular AA profile in K-Ras/PI3K cells showed a poor correlation with plasma free AA profiles previously obtained from breast cancer patients,[13,18] the integration of intracellular and extracellular AA profiles with AA-associated pathways for the identical cancer tissue will contribute to disclose the cancer-specific AA metabolism.

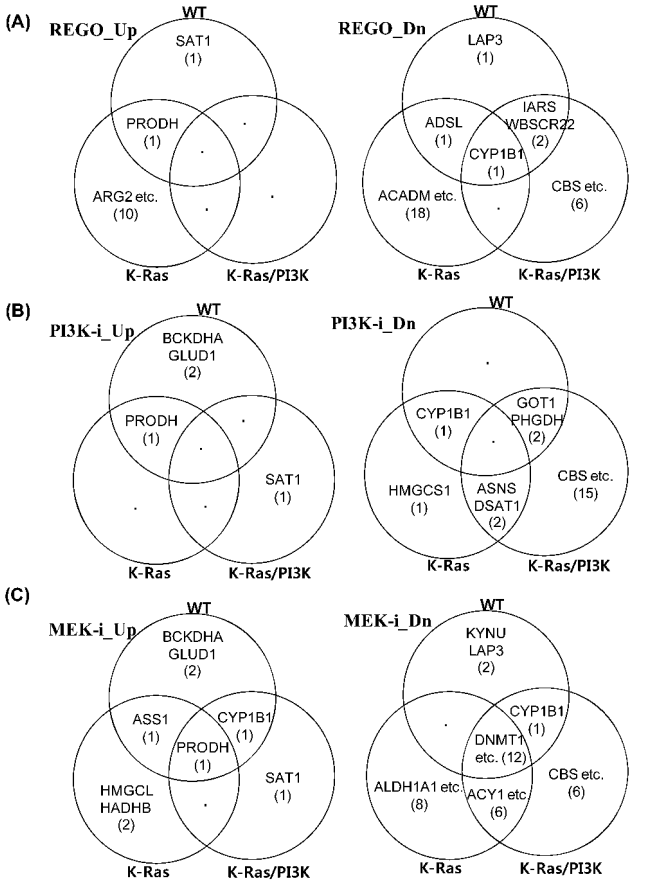

Fig. 6 Enzymes with significant changes in the corresponding transcript levels under inhibitor treatments. (A) Upregulated and downregulated gene transcripts under REGO treatment. (B) Upregulated and downregulated gene transcripts under PI3K-i treatment. (C) Upregulated and downregulated gene transcripts under MEK-i treatment.

Conclusions

We analyzed the intracellular free AA level and the transcript level of AA-associated enzymes in human isogenic mammary epithelial cells expressing K-Ras and PI3K mutant oncogenes and treated with kinase inhibitors. On one hand, the changes in AA levels detected in these isogenic cells, recapitulating the oncogene transformation in breast cancer, may suggest an additional biomarker for patient stratification. On the other hand, the differential regulation of AA and transcript levels induced by the kinase inhibitors appears to correlate with the oncogene pathways activated in the respective cell lines. Thus, this observation might support future combination therapy of kinase inhibitors and novel drug targeting enzymes of AA pathways.

Acknowledgements

We gratefully acknowledge the Bayer Health Care (BMSI/10-3004B-SBIC) for financial support.

References

1 D. Hanahan and R. A. Weinberg, *Cell*, 2011, **144**, 646–674.
2 J. R. Cantor and D. M. Sabatini, *Cancer Discovery*, 2012, **2**, 881–898.
3 W. H. Koppenol, P. L. Bounds and C. V. Dang, *Nat. Rev. Cancer*, 2011, **11**, 325–337.
4 R. A. Cairns, I. S. Harris and T. W. Mak, *Nat. Rev. Cancer*, 2011, **11**, 85–95.
5 M. G. Vander Heiden, L. C. Cantley and C. B. Thompson, *Science*, 2009, **324**, 1029–1033.
6 G. Kroemer and J. Pouyssegur, *Cancer Cell*, 2008, **13**, 472–482.
7 A. J. Levine and A. M. Puzio-Kuter, *Science*, 2010, **330**, 1340–1344.
8 Y. Zhao, E. B. Butler and M. Tan, *Cell Death Dis.*, 2013, **4**, e532.
9 R. M. Vabulas and F. U. Hartl, *Science*, 2005, **310**, 1960–1963.
10 J. Onodera and Y. Ohsumi, *J. Biol. Chem.*, 2005, **280**, 31582–31586.
11 A. Efeyan, R. Zoncu and D. M. Sabatini, *Trends Mol. Med.*, 2012, **18**, 524–533.
12 H. S. Lai, J. C. Lee, P. H. Lee, S. T. Wang and W. J. Chen, *Semin. Cancer Biol.*, 2005, **15**, 267–276.
13 Y. Miyagi, M. Higashiyama, A. Gochi, M. Akaike, T. Ishikawa, T. Miura, N. Saruki, E. Bando, H. Kimura and F. Imamura, *PLoS One*, 2011, **6**, e24143.
14 T. J. Wang, M. G. Larson, R. S. Vasan, S. Cheng, E. P. Rhee, E. McCabe, G. D. Lewis, C. S. Fox, P. F. Jacques and C. Fernandez, *Nat. Med.*, 2011, **17**, 448–453.
15 K. Hiller and C. M. Metallo, *Curr. Opin. Biotechnol.*, 2013, **24**, 60–68.
16 H. S. Lai, J. C. Lee, P. H. Lee, S. T. Wang and W. J. Chen, *Semin. Cancer Biol.*, 2005, **15**, 267–276.
17 J. R. Mayers, C. Wu, C. B. Clish, P. Kraft, M. E. Torrence and B. P. Fiske, *Nat. Med.*, 2014, **20**, 1193–1198.
18 Y. Gu, T. Chen, S. Fu, X. Sun, L. Wang, J. Wang, Y. Lu, S. Ding, G. Ruan, L. Teng and M. Wang, *J. Transl. Med.*, 2015, **13**, 1–14.
19 N. Fukutake, M. Ueno, N. Hiraoka, K. Shimada, K. Shiraishi, N. Saruki, T. Ito, M. Yamakado, N. Ono, A. Imaizumi, S. Kikichi, H. Yamamoto and K. Katayama, *PLoS One*, 2015, **10**(7), e0132223.
20 F. Cheng, Z. Wang, Y. Huang, Y. Duan and x. Wang, *Clin. Chim. Acta*, 2015, **447**, 23–31.
21 X. F. Han, Y. Q. Liu, L. X. Wang, Q. X. Yang and H. B. Xiao, *Biotechnol. Lett.*, 2012, **34**, 1–7.
22 H. Konishi, B. Karakas, A. M. Abukhdeir, J. Lauring, J. P. Gustin, J. P. Garay, Y. Konishi, E. Gallmeier, K. E. Bachman and B. H. Park, *Cancer Res.*, 2007, **67**, 8460–8467.
23 S. Arena, C. Isella, M. Martini, A. de Marco, E. Medico and A. Bardelli, *Cancer Res.*, 2007, **67**, 8468–8476.
24 E. Castellano and J. Downward, *Genes Cancer*, 2011, **2**, 261–274.
25 J. P. Gustin, B. Karakas, M. B. Weiss, A. M. Abukhdeir, J. Lauring, J. P. Garay, D. Cosgrove, A. Tamaki, H. Konishi and Y. Konishi, *Proc. Natl. Acad. Sci. U. S. A.*, 2009, **106**, 2835–2840.
26 R. Schmieder, J. Hoffmann, M. Becker, A. Bhargava, T. Muller, N. Kahmann, P. Ellinghaus, R. Adams, A. Rosenthal and K. H. Thierauch, *Int. J. Cancer*, 2014, **135**, 1487–1496.
27 I. V. Hartung, M. Hitchcock, F. Puhler, R. Neuhaus, A. Scholz, S. Hammer, K. Petersen, G. Siemeister, D. Brittain and R. C. Hillig, *Bioorg. Med. Chem. Lett.*, 2013, **23**, 2384–2390.
28 C. A. Sellick, R. Hansen, G. M. Stephens, R. Goodacre and A. J. Dickson, *Nat. Protoc.*, 2011, **6**, 1241–1249.